



ELSEVIER

Journal of Crystal Growth 237–239 (2002) 858–863

JOURNAL OF  
**CRYSTAL  
GROWTH**

www.elsevier.com/locate/jcrysgr

# Growth of Co-doped (Ba,Sr)TiO<sub>3</sub> single crystals and their characterization

S. Madeswaran, N.V. Giridharan, R. Jayavel\*, C. Subramanian

*Crystal Growth Centre, Anna University, Chennai 600 025, Tamil Nadu, India*

## Abstract

Single crystals of Co-doped B<sub>1-x</sub>Sr<sub>x</sub>TiO<sub>3</sub> (Co:BST) have been grown by high-temperature solution growth technique. The dopant has significant effect on the growth parameters and considerably reduced the twin formation in the grown crystal. Bulk single crystals of dimensions 5 × 5 × 4 mm<sup>3</sup> have been grown with optimized growth parameters. Layer growth and vein-like structure patterns, indicative of 2D nucleation mechanism, have been observed on the grown crystals. The presence of dopant in the grown crystals was confirmed by EDX analysis. For lower doping concentration (0.1 mol%), the crystal possesses tetragonal structure and changes to cubic for higher dopant level (1 and 5 mol%) Co doping in BST increases the dielectric constant values and decreases the Curie temperature (*T<sub>c</sub>*). The spontaneous polarization (*P<sub>s</sub>*) value for 0.1 mol% of Co-doped BST crystal is measured to be 22 μC/cm<sup>2</sup> and the value decreases with increasing Co concentration. © 2002 Elsevier Science B.V. All rights reserved.

*PACS:* 77.84.-s; 77.80.-e; 77.22.Ch; 77.80.Dj; 74.25.Gz

*Keywords:* A2. Growth from high-temperature solutions; B2. Ferroelectric materials

## 1. Introduction

In recent years, there has been increasing interest on photorefractive materials, which are known to be promising candidates for high-resolution and high-fidelity holographic memories [1,2]. The possibility of obtaining high non-linearity at milli-watt power level makes these materials attractive for applications in optical signal processing, dynamic holography and self-pumped phase conjugation. Among the variety of photorefractive materials available, perovskite

BaTiO<sub>3</sub> is one of the promising candidates, due to its extremely large electro-optic coefficient and high holographic sensitivity [3]. However, their slow response time seriously limit the potentiality for photorefractive applications. There have been several investigations to improve the photorefractive and ferroelectric properties by suitable doping in BaTiO<sub>3</sub> [4,5]. It has been reported that Co doping in BaTiO<sub>3</sub> enhances the photorefractive properties [6,7]. However, growth of pure BaTiO<sub>3</sub> by flux growth resulted in twinned and platy crystals [8,9]. Instead, partial substitution of Sr in BaTiO<sub>3</sub> (B<sub>1-x</sub>Sr<sub>x</sub>TiO<sub>3</sub>) yielded bulk crystals with large pyroelectric coefficient at room temperature [10,11]. Growth aspects of Ce- and Nd-doped BST have already been studied in our earlier reports

\*Corresponding author. Tel.: +91-144-235-2774; fax: +91-144-235-2870.

*E-mail address:* rjvel@hotmail.com (R. Jayavel).

[12,13]. In the present investigation, with the aim of growing bulk single crystals with improved pyroelectric and photorefractive properties, Co-doped  $B_{1-x}Sr_xTiO_3$  (Co:BST) has been attempted for the first time. Structural, optical and ferroelectric properties of the Co-doped BST crystals have also been reported.

## 2. Experiments

High-purity  $BaCO_3$  (99.98%),  $SrCO_3$  (99.995%),  $TiO_2$  (99.99%) and  $CoO_3$  (99%) were used for the growth of Co:BST single crystals with different dopant concentrations at a fixed Sr concentration of 20 mol%. The powders were mixed in the appropriate ratio and calcined at  $1100^\circ C$  for 10 h. The calcined powder was taken in a  $100\text{ cm}^3$  platinum crucible and mixed with KF flux in the required flux-charge ratio. The crucible was tightly closed to avoid the evaporation of flux and loaded into a vertical-type silicon carbide furnace controlled by a Eurotherm (model 818) temperature controller with an accuracy of  $\pm 1^\circ C$ . The furnace was heated from  $1190^\circ C$  up to  $1225^\circ C$  depending on the dopant concentration, homogenized for 10–20 h and then slow cooled to  $800^\circ C$  at a rate of  $1\text{--}5^\circ C/h$ . Finally, the furnace was cooled down to room temperature at a faster rate ( $50^\circ C/h$ ). The grown crystals were separated from the flux by dissolving in hot distilled water. The growth parameters were optimized to grow large size crystals by varying the flux-charge ratio, cooling rate and soaking period. The optimized growth conditions are given in Table 1. Bulk crystals of equidimensional morphology were grown by step-cooling process using the following

growth cycle:

$$\begin{aligned} &RT \xrightarrow{75^\circ C/h} 1190\text{--}1220^\circ C \xrightarrow{10\text{--}20\text{ h}} 1190\text{--}1220^\circ C \\ &\xrightarrow{1^\circ C/h} 1050^\circ C \xrightarrow{10\text{ h}} 1050^\circ C \xrightarrow{2^\circ C/h} 900^\circ C \\ &\xrightarrow{5\text{ h}} 900^\circ C \xrightarrow{5^\circ C/h} 800^\circ C \xrightarrow{50^\circ C/h} RT. \end{aligned}$$

Most of the crystals were found at the bottom of the crucible. Bulk crystals of size  $5 \times 5 \times 4\text{ mm}^3$ , without butterfly twins, were grown for the dopant concentrations of 0.1 and 1 mol%. Growth mechanism and surface morphology of the crystals were studied with an optical microscope in the reflection mode. XRD patterns were recorded by using Rich Seift diffractometer with  $Cu\ K_\alpha$  ( $\lambda = 1.5418\text{ \AA}$ ) radiation. Dielectric measurements and hysteresis loop studies were carried out using impedance analyzer and modified Sawyer–Tower circuit, respectively.

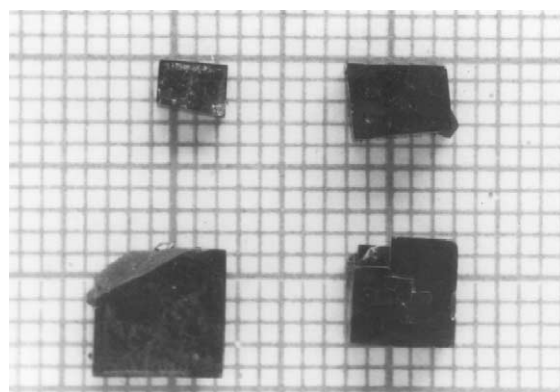


Fig. 1. As-grown Co-doped BST single crystals.

Table 1  
Growth parameters, lattice constants and Curie temperature for different dopant concentrations of Co:BST single crystals

Composition (mol%)	Flux-charge ratio	Soaking period (h)/cooling rate ( $^\circ C/h$ )	Growth temperature ( $^\circ C$ )	Lattice parameter		$T_c$ ( $^\circ C$ )
				$a$ ( $\text{\AA}$ )	$c$ ( $\text{\AA}$ )	
BST:Co—0.1	80:20	12/5	1190	4.0085	4.0175	52
BST:Co—1.0	80:20	15/3	1200	4.0144	4.0144	27
BST:Co—5.0	82:17	20/1	1220	4.0168	4.0168	<RT

### 3. Result and discussion

#### 3.1. Crystal growth

Initial growth runs with faster cooling rate and minimum soaking period resulted in dendritic

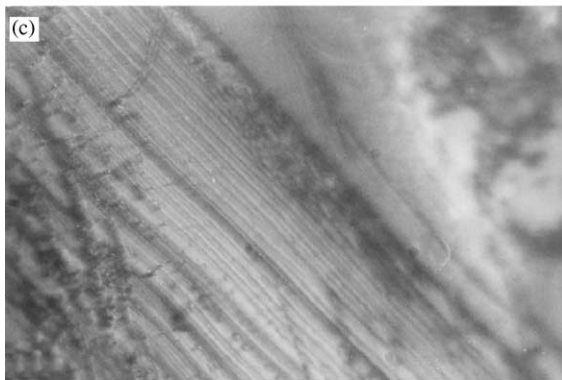


Fig. 2. Surface morphology of Co:BST single crystals: (a) vein-like structure, (b) layer growth pattern and (c) vein structure with two-dimensional growth.

growth, yielding crystals with lot of flux inclusions. Slow growth rate increased the size and quality of the crystals. The butterfly twinning was completely reduced owing to the inhibition of hexagonal phase at high temperature, which controls (111) twinning during nucleation [9]. Solubility was found to decrease with increase of Co content and hence the flux ratio was increased for higher dopant concentration. After repeated growth runs, the flux ratio was optimized to grow equidimensional crystals for each composition as given in Table 1. Fig. 1 shows the as-grown Co-doped BST single crystals. The EDX measurements reveal that the dopant concentration in the grown crystals is slightly lower than the initial concentration.

#### 3.2. Surface morphology

Fig. 2a exhibits the surface morphology of Co-doped BST single crystals with a vein-like structure. In flux growth, surface morphology of the crystal depends on the supersaturation, cooling rate and growth mechanism. The vein-like structure is formed due to growth below 1000°C, at a

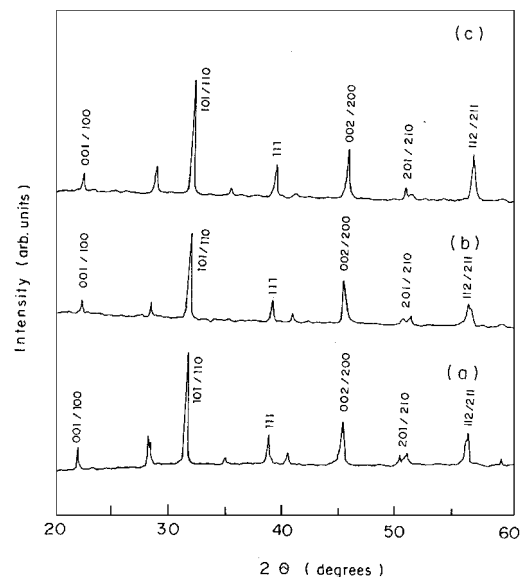


Fig. 3. X-ray diffraction pattern of Co:BST with (a) 0.1 mol% (b) 1 mol% and (c) 5 mol% of Co.

lower supersaturation and low stacking fault energy, as observed generally in  $\text{BaTiO}_3$  family crystals [9,12]. Layer growth pattern has been clearly observed at the edge of the crystals (Fig. 2b), indicative of two-dimensional nucleation mechanism [13]. After the formation of vein-like structure, the gap between the arms is filled by two-dimensional growth and simultaneous arms spreading occurs as shown in Fig. 2c. It has been observed that the spreading of arms increases and the arms are far separated as they reach the edge.

### 3.3. Structural and optical property studies

Figs. 3a–c show the powder X-ray diffraction patterns of Co:BST crystals grown with 0.1, 1 and 5 mol% of Co, respectively. The crystals possess tetragonal structure for lower doping level (0.1 mol%). For higher doping concentrations (1 and 5 mol%), structure shifts to cubic phase. The lattice parameter values for the different concentrations of Co are given in Table 1. The transmission and absorption spectra were recorded for 0.1 and 1 mol% of Co-doped BST crystals after

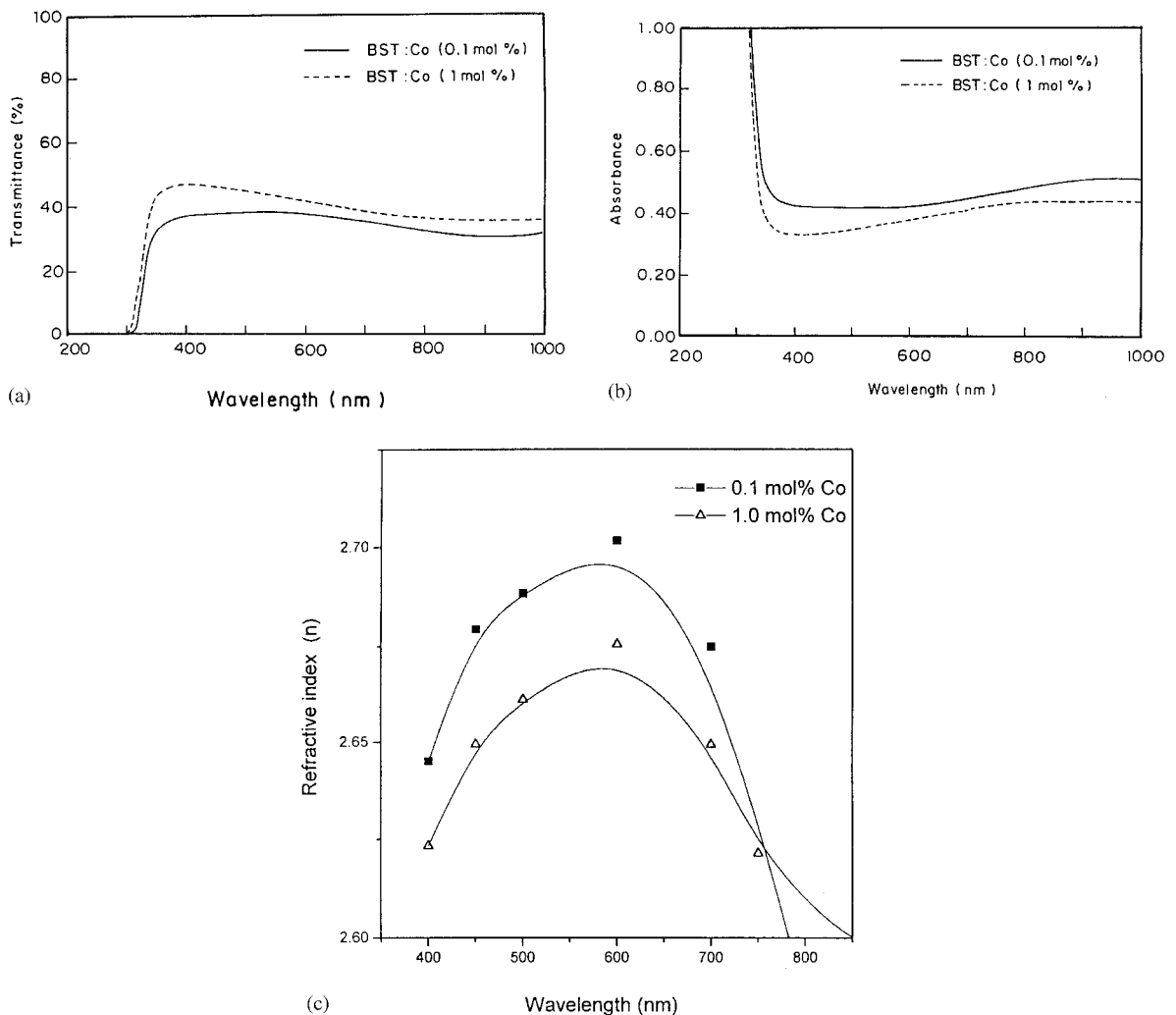


Fig. 4. The optical properties of Co:BST single crystal: (a) transmission spectra, (b) absorption spectra and (c) refractive index with respect to wavelength.

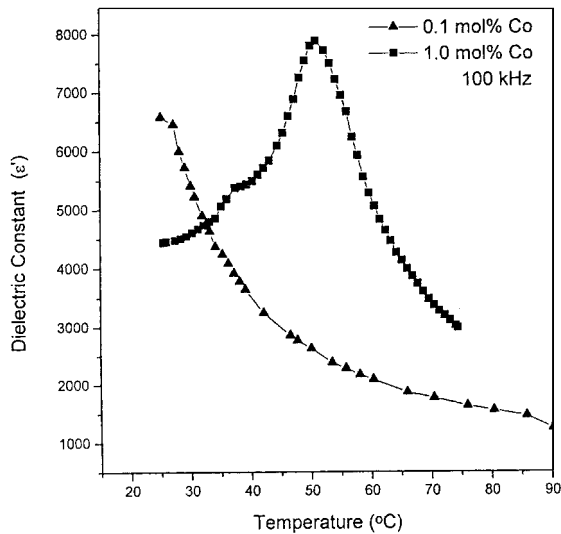


Fig. 5. Dielectric constant vs. temperature for (a) 0.1, and (b) 1 mol% of Co-doped BST single crystals.

lapping into 1.5 mm thickness and polished with a 6  $\mu\text{m}$  diamond paste. The transmission and absorption spectra are shown in Fig. 4a and b, respectively. From the spectra, refractive index values were calculated for various wavelengths using the formula

$$n = \frac{(1 + R^{1/2})}{(1 - R^{1/2})},$$

where  $R$  is the reflectance. The refractive index values depicted in Fig. 4c are comparable with the value of pure  $\text{BaTiO}_3$  (2.66).

### 3.4. Ferroelectric properties

The dielectric constants were measured at 100 kHz for the Co:BST single crystals at different temperatures. Dielectric constant vs. temperature for 0.1, and 1 mol% of Co-doped BST single crystals are shown in Fig. 5a and b, respectively. The Curie temperature ( $T_c$ ) decreases and reaches to room temperature for 1 mol% of Co and the values are given in Table 1. The decrease in  $T_c$  is attributed to the distortion in lattice (structure changes from tetragonal to cubic) as revealed by XRD studies and the change is in the reverse order compared to Ce-doped BST crystals [12]. The

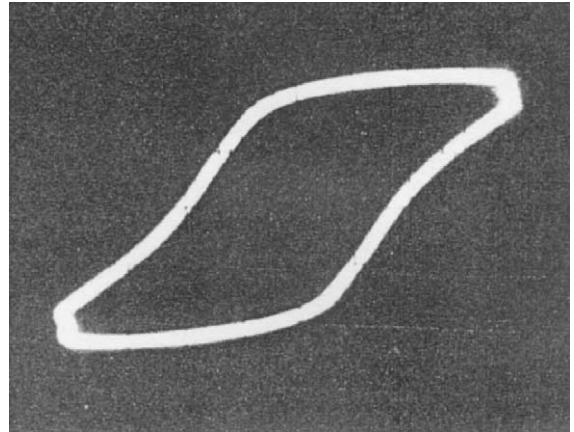


Fig. 6. Hysteresis loop of Co:BST single crystals grown with 0.1 mol% of Co.

dielectric constant increases with a maximum value at Curie temperature. For 0.1 mol% of Co, the dielectric constant is measured to be 8000, which is one and half times higher than that of undoped BST single crystals. Also it is interesting to note that the diffused nature decreased and the phase transition becomes sharp. Fig. 6 presents the hysteresis structure of Co:BST single crystals grown with 0.1 mol% of Co. The hysteresis was traced at room temperature without poling the crystal. The spontaneous polarization ( $P_s$ ) value for 0.1 mol% Co-doped BST crystal is measured to be 22  $\mu\text{C}/\text{cm}^2$  and the value decreases with increasing Co concentration.

### 4. Conclusion

Growth aspects of Co-doped BST single crystals have been studied. The dopant has significant effect on the growth temperature, morphology, soaking period and cooling rate. Bulk crystals of size  $5 \times 5 \times 4 \text{ mm}^3$  without butterfly twins, suitable for photorefractive property studies, have been grown with optimized growth parameters. The change in crystal structure from tetragonal to cubic leads to a decrease in Curie temperature for Co-doped BST crystals. For 0.1 mol% of Co, the dielectric constant increases sharply at room temperature, indicating the absence of diffused

phase transition. It is concluded that Co doping in BST yields bulk single crystals with promising ferroelectric properties.

## References

- [1] F.H. Mok, M.C. Tackitt, H.M. Stoll, *Opt. Lett.* 16 (1991) 605.
- [2] D. Psaltis, F.H. Mok, H.S. Li, *Opt. Lett.* 19 (1994) 210.
- [3] J. Zhuang, G.S. Li, X.C. Gao, X.B. Guo, Y.H. Huang, Z.Z. Shi, Y.Y. Weng, J. Lu, *Opt. Commun.* 82 (1991) 69.
- [4] A.R. Johnston, *J. Appl. Phys.* 42 (1971) 3501.
- [5] M.B. Klein, R.N. Schwartz, *J. Opt. Soc. Am. B* 3 (1986) 293.
- [6] S. Shmuel, Y. Glicks, *Opt. Lett.* 20 (1995) 2369.
- [7] P. Mathey, P. Jullien, P. Lompre, D. Rytz, *Appl. Phys. A* 66 (1998) 511.
- [8] R.C. Bradt, G.S. Ansell, *Mater. Res. Bull.* 2 (1967) 585.
- [9] S. Balakumar, R. Ilangovan, S. Ganesa Moorthy, C. Subramanian, *Mater. Res. Bull.* 30 (1995) 587.
- [10] D. Rytz, B.A. Wechler, M.H. Garrett, C.C. Nelson, R.N. Schwartz, *J. Opt. Soc. Am. B* 7 (1990) 2245.
- [11] J. Furukawa, T. Tsukamoto, *Jpn. J. Appl. Phys.* 30 (1991) 2391.
- [12] R. Varatharajan, R. Jayavel, C. Subramanian, P. Ramasamy, *Mater. Res. Bull.* 35 (1999) 603.
- [13] R. Varatharajan, S. Madeswaran, R. Jayavel, *J. Crystal Growth* 225 (2001) 484.